

Theoretical analysis of element 120 synthesized in the $^{58}\text{Fe} + ^{244}\text{Pu}$ hot fusion reaction

Yu-Jie Liang,^{1,*} Min Zhu,¹ Zu-Hua Liu,² and Wen-Zhong Wang¹

¹*School of Science, Minzu University of China, Beijing 100081, People's Republic of China*

²*China Institute of Atomic Energy, Beijing 102413, People's Republic of China*

(Received 16 July 2012; revised manuscript received 30 August 2012; published 17 September 2012)

Synthesis of element 120 in the $^{58}\text{Fe} + ^{244}\text{Pu}$ hot fusion reaction has been evaluated by means of a modified “fusion by diffusion” (FBD) model. In the model, dynamic evolution from dinucleus to mononucleus is taken into account with the two-dimensional coupled Langenvin equations. The calculated maximum evaporation residue cross sections in $3n$ - and $4n$ -evaporation channels of $^{58}\text{Fe} + ^{244}\text{Pu}$ reaction are 0.005 and 0.016 pb, which are far below the present experimental sensitivity for the detection of one decay. The fusion probability calculated with the modified FBD model clearly shows that fusion of the heavy system $^{58}\text{Fe} + ^{244}\text{Pu}$ is severely hindered.

DOI: [10.1103/PhysRevC.86.037602](https://doi.org/10.1103/PhysRevC.86.037602)

PACS number(s): 24.10.-i, 24.60.-k, 25.70.Jj, 27.90.+b

During recent years, significant progress has been made experimentally in the synthesis of superheavy elements (SHEs). Isotopes with $Z \leq 113$ and $N \leq 165$ were synthesized [1,2] by means of the cold fusion reaction involving ^{208}Pb and ^{209}Bi targets and stable neutron-rich heavy projectiles. On the other hand, reactions of doubly magic ^{48}Ca projectiles with actinide targets have been used for the synthesis of elements with $Z \geq 112$. These reactions, termed hot fusion, led to the observation of isotopes with $Z = 112$ – 118 [3–8]. So far, these experimental results have provided clear evidence of the existence of an island of stability in the region of superheavy nuclei.

However, there is still an open question as to where the center of the island of stability is located. All advanced nuclear structure models [9–12] predict neutron shell closure at $N = 184$, while there is no common conclusion about the next magic proton number among the different models. The macro-microscopic nuclear model predicts the magic proton shell at $Z = 114$ [9,10]. Nevertheless, the microscopic Hartree-Fock-Bogoliubov and relativistic mean-field theories suggest that the magic proton shell should be at higher proton numbers, $Z = 120$ – 126 [11,12]. Therefore, synthesis of new SHEs with $Z \geq 120$ is of great interest theoretically. On the experimental side, because californium is the heaviest actinide that can be used as a target material in hot fusion reactions, experiments in terms of reactions with projectiles heavier than ^{48}Ca have to be carried out for the synthesis of SHEs with $Z \geq 120$. To this end, detailed investigation on actinide-based complete fusion reactions with stable neutron-rich projectiles as heavy as ^{58}Fe or ^{64}Ni is of great importance.

Recently, Oganessian *et al.* [13] performed an experiment aimed at the synthesis of isotopes of element 120 using the $^{244}\text{Pu}(^{58}\text{Fe},xn)^{302-x}120$ reaction. Decay chains that could be assigned to the isotopes of element 120 or its daughter nuclei were not observed in their experiment. The sensitivity of the experiment corresponds to a cross section of 0.4 pb for the detection of one decay. In this work, we make a detailed analysis of that reaction by means of the “fusion by diffusion” (FBD) model [14–18] with the purpose of being helpful in

future experiments to produce SHEs with $Z \geq 120$ using heavier projectiles. In addition, in order to check the reliability of our approach we have also evaluated the evaporation residue (ER) cross sections of the $^{238}\text{U}(^{48}\text{Ca},xn)^{286-x}112$ reaction and compared them with the experimental data.

The cross section of a superheavy nucleus produced in a heavy-ion fusion-evaporation reaction is calculated as follows:

$$\sigma_{\text{ER}}(E_{\text{c.m.}}) = \pi \lambda^2 \sum_{l=0}^{\infty} (2l+1) P_{\text{capt}}(E_{\text{c.m.}}, l) P_{\text{fus}}(E_{\text{c.m.}}, l) \times P_{xn}(E_{\text{c.m.}}, l). \quad (1)$$

Here P_{capt} is the capture probability of the colliding nuclei after overcoming the Coulomb barrier and moving up to the contact point. We calculate P_{capt} by means of a semiphenomenological barrier distribution function method proposed by Zagrebaev *et al.* [19,20]. P_{fus} defines the probability that the system will go from the configuration of two nuclei in contact to the configuration of a compound nucleus (CN). We use the modified FBD model [17,18] to evaluate the CN formation probability P_{fus} . In the modified FBD model, evolution from dinucleus to mononucleus is taken into account. As pointed out by Boilley *et al.* [21], the neck dynamics has an important influence on the fusion of heavy nuclei. Finally, P_{xn} represents the survival probability of the excited CN after evaporation of x neutrons in the cooling process.

The orientation effects of deformed nuclei play an important role in sub-barrier fusion. The dynamical deformations of the projectile and target in the entrance channel have been included in the dinuclear system model [22–25] with a specified orientation (e.g., a tip-tip orientation of the two deformed nuclei in Ref. [25]). In two publications, the arbitrarily oriented deformed potentials have been calculated for lighter reaction systems [26,27]. However, to our knowledge, such calculations have not yet been applied to the dynamic investigation of superheavy nuclei formation. The main difficulty here stems from the lack of knowledge about the subsequent dynamic evolution of nuclear shapes after two nuclei make contact [28]. Besides, the effects of static deformation of the target nucleus on the capture [29] and fusion probabilities [30] at least partially cancel each other as far as the ER cross sections are concerned. For simplicity, target deformation is not taken

*lyj85@126.com

into account in dynamic simulations, and the shape of the system is specified in terms of two spheres with radii R_1 and R_2 smoothly connected by a hyperboloidal neck [15,31]. Three variables may be defined for a given shape: elongation, mass asymmetry, and neck size (n). Instead of elongation, we use s , namely, the separation between the surfaces of approaching nuclei. We assume that neutron-proton equilibrium is achieved at the contact point and mass asymmetry is fixed thereafter. We describe the dynamic evolution from a dinucleus (in the fusion valley) to a mononucleus (in the asymmetric fission valley) by means of a two-dimensional coupled Langevin equation,

$$\begin{aligned} \frac{dq_i}{dt} &= \mu_{ij} p_j, \\ \frac{dp_i}{dt} &= -\frac{1}{2} p_j p_k \frac{\partial \mu_{jk}}{\partial q_i} - \frac{\partial V(q)}{\partial q_i} - \gamma_{ij} \mu_{jk} p_k + \theta_{ij} \xi_j(t), \end{aligned} \quad (2)$$

where $q_i \equiv s, n$ stand for the collective coordinates, p_i are its conjugate momenta, $V(q)$ is the nuclear deformation potential calculated in the framework of the finite-range liquid drop model [32,33], μ_{ij} ($i, j \equiv s, n$; the same for the other quantities below) denotes the inverse matrix elements of the inertia tensor m_{ij} , and γ_{ij} is the friction tensor calculated with the one-body dissipation model [17,34–37]. The normalized random variables ξ_j are assumed to be independent white noises. The strength θ_{ij} of the random force is given by $\theta_{ik}\theta_{kj} = T\gamma_{ij}$, with T the temperature of the heat bath, which is calculated along each trajectory [38] from the internal excitation energy E^* and the level density parameter a by the Fermi gas relation,

$$T = \sqrt{E^*/a}. \quad (3)$$

The inertia tensor m_{ij} was evaluated under the Werner-Wheeler approximation [31,39] for incompressible and irrotational flow.

The treatment of the connection between two steps is a subtle problem that can change the final results [21]. Basically, the initial conditions for the second step play a role in this kind of connection [40]. There are twofold effects of the initial conditions on the ER cross sections. First, the initial condition will influence the injection configuration in the asymmetric fission valley, which brings about a change of the inner barrier (saddle-point) height. Because the fusion probability almost exponentially depends on the inner barrier height, this will dramatically change the fusion probability. Second, the formation cross sections of superheavy nuclei are mainly determined by the production of the fusion and survival probabilities. The former factor increases, while the latter one exponentially decreases, with increasing excitation energy [15]. Therefore, a change in the fusion probability will cause variance of the peak position of the excitation function, which results in a change in the ER probability. For example, if the system is injected into the asymmetric fission valley with a more elongated shape, the inner barrier height will be increased, resulting in a dramatic decrease in the fusion probability and somehow push the peak of the excitation function to a higher excitation energy. Consequently, the ER probability will exponentially decrease. From the above discussion, one may see that the final results are very sensitive to the initial

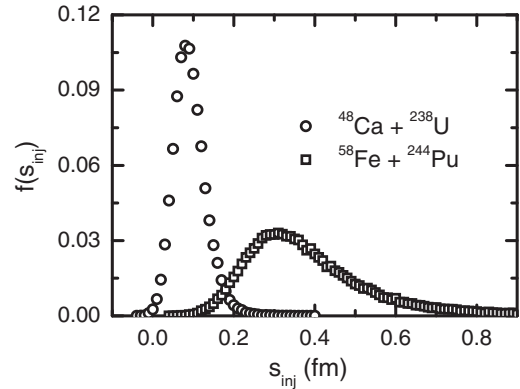


FIG. 1. Probability distributions of s_{inj} calculated with coupled Langevin equations for the systems $^{48}\text{Ca} + ^{238}\text{U}$ (open circles) and $^{58}\text{Fe} + ^{244}\text{Pu}$ (open squares) at a CN excitation energy of 40 MeV.

conditions, which should be treated carefully. In the present work, the initial conditions for the radial and neck motions defined in Refs. [16,17] are adopted. Similarly to the criterion suggested by Swiatecki [41], we define $n = \sqrt{0.5}R_i$, with $R_i = \min(R_1, R_2)$ the boundary between the dinuclear and the mononuclear regimes. By solving these dynamic equations we obtain the probability distributions of the radial degrees of freedom at the injection point s_{inj} in the asymmetric fission valley. As an example, the resultant distributions $f(s_{\text{inj}})$ are plotted in Fig. 1 for the systems $^{48}\text{Ca} + ^{238}\text{U}$ and $^{58}\text{Fe} + ^{244}\text{Pu}$ at the CN excitation energy $E^* = 40$ MeV. Here, s_{inj} is the distance between the surfaces of two approaching nuclei where injection into the asymmetric fission valley takes place.

After injection into the asymmetric fission valley, thermal shape fluctuations in the valley can occasionally bring the system over the saddle point. In the case of one-dimensional diffusion over a parabolic barrier, the probability arrived at for the CN configuration is [14,15,18]

$$P_{\text{fus}}(E_{\text{c.m.}}, l) = \frac{1}{2} \text{erfc}(\sqrt{B(l)/T}), \quad (4)$$

where T is the temperature of the fusing system, which we take as the mean value of the initial temperature at injection point T_{inj} and the temperature at the top of the saddle point T_{saddle} . $B(l)$ is the barrier height measured from the injection point, which consists of the macroscopic deformation energy ΔE ($l = 0$) and rotational energy $\Delta E^{\text{rot}}(l)$ in the l -dependent FBD model [18]. The macroscopic deformation energy along the asymmetric fission valley is calculated using the refined algebraic expressions [18]. The corresponding values of the rotational energy at the injection point and at the symmetric saddle point are calculated with moments of inertia specified in Ref. [18]. In our approach, the stochastic nature of neck growth process results in a distribution $f(s_{\text{inj}})$ of the injection point. As the barrier height is measured from the injection point s_{inj} , this brings about the height of the barrier $B(s_{\text{inj}}, l)$ a relevant distribution. Therefore, the fusion probability takes the form

$$P_{\text{fus}}(E_{\text{c.m.}}, l) = \frac{1}{2} \int \text{erfc}(\sqrt{B(s_{\text{inj}}, l)/T}) f(s_{\text{inj}}) ds_{\text{inj}}. \quad (5)$$

Displayed in Fig. 2 are the fusion probabilities as a function of angular momentum for the systems $^{48}\text{Ca} + ^{238}\text{U}$ and

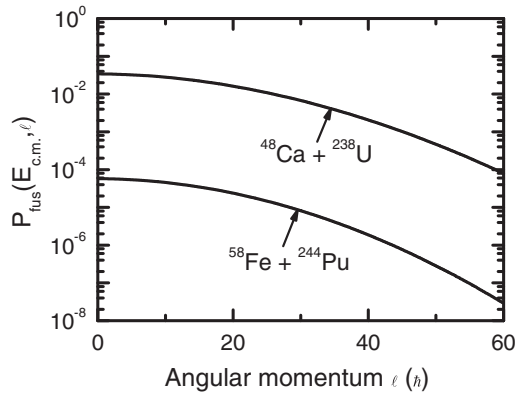


FIG. 2. Fusion probabilities as a function of angular momentum for the systems $^{48}\text{Ca} + ^{238}\text{U}$ and $^{58}\text{Fe} + ^{244}\text{Pu}$ at the CN excitation energy $E^* = 40$ MeV.

$^{58}\text{Fe} + ^{244}\text{Pu}$ at the CN excitation energy $E^* = 40$ MeV. It is shown in the figure that the fusion probability of the latter system is about three orders of magnitude smaller than that of the former one, which means that fusion is severely hindered for heavy reaction systems such as $^{58}\text{Fe} + ^{244}\text{Pu}$.

We calculate the last factor P_{xn} by a more or less convenient method; for details see Ref. [42]. The essential ingredient in the formalism is the ratio of the partial widths of neutron emission (Γ_n) and fission (Γ_f) for the nucleus after the emission of k neutrons [42–44],

$$\frac{\Gamma_n(E_k^*, l_k)}{\Gamma_f(E_k^*, l_k)} = \frac{4A^{2/3}a_f U_n^{\max}(k)}{K_0 a_n [2\sqrt{a_f U_f^{\max}(k)} - 1]} \times \exp[2\sqrt{a_n U_n^{\max}(k)} - 2\sqrt{a_f U_f^{\max}(k)}], \quad (6)$$

where A is the mass number of the nucleus considered, $K_0 = \hbar^2/[2m_n r_0^2] \simeq 9.8$ MeV, with m_n and r_0 the neutron mass and nuclear radius, and a_n and a_f are the level density parameters of the daughter nucleus and the fissioning nucleus in the ground and saddle configurations, respectively. $U_n^{\max}(k)$ and $U_f^{\max}(k)$ [44] denote the upper limit of the thermal excitation energies of the $(k+1)$ th daughter nucleus in the ground state and nucleus at the saddle point after the emission of k neutrons. In the calculations of these excitation energies, data on the microscopic shell correction $\Delta_{\text{sh}}^{\text{gs}}$ in the ground state and the neutron separation energy are taken from Ref. [9], and the macroscopic deformation energies B_{LD} are set to 0 [44,45]. The shape-dependent level density parameter is given by the expression [15]

$$\tilde{a} = 0.076A + 0.180A^{2/3}F(\alpha) + 0.157A^{1/3}G(\alpha) \text{ MeV}^{-1}, \quad (7)$$

where the deformation of the nucleus is defined by the parameter $\alpha = (R_{\text{max}} - R)/R$, where R_{max} is the semimajor axis of the nucleus with its radius R before deformation. The functions F and G are given in Ref. [15]. The smooth value of the level density parameter \tilde{a} is modified owing to shell effects according to the formula [44,46]

$$a = \tilde{a} \left[1 + \frac{\Delta_{\text{sh}}}{U} (1 - \exp(-U/E_d)) \right], \quad (8)$$

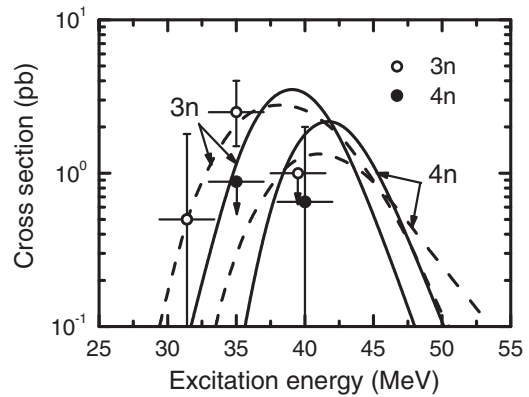


FIG. 3. Excitation functions for the $3n$ and $4n$ evaporation channels from the complete fusion reaction $^{48}\text{Ca} + ^{238}\text{U}$. Solid and dashed lines are the predictions of the present work and Zagrebaev *et al.* [48], respectively. Experimental data are taken from Ref. [5].

where E_D is the damping parameter describing the decrease in the influence of shell effects on the energy level density with increasing excitation energy U of the nucleus. In this work, $E_D = 18.5$ MeV [44,47] is used. Siwek-Wilczyńska and Skwira [44] presented a systematics of the shell corrections at the saddle point $\Delta_{\text{sh}}^{\text{sd}}$ deduced from experimental fission excitation functions for a wide range of nuclei of $88 \leq Z \leq 100$. Their systematics show that the values of $\Delta_{\text{sh}}^{\text{sd}}$ are close to 0 for nuclei with $Z \geq 100$. Therefore, in the range of superheavy nuclei, the level density parameters a_f can be safely assumed to be independent of the excitation energy of the nucleus considered. On the other hand, the level density parameter a_n increases as the excitation energy increases owing to the damping of the shell correction energy $\Delta_{\text{sh}}^{\text{gs}}$ of the ground state. Therefore, according to the formalism presented in Refs. [14,15,44], the damping of the shell effects directly influences the decay width of neutron emission Γ_n rather than the fission width Γ_f .

With the model described above, we first evaluated the ER cross sections for the $^{48}\text{Ca} + ^{238}\text{U}$ hot fusion reaction and compare the results with the experimental data [5] in Fig. 3. The dashed lines in the figure are the prediction of Zagrebaev *et al.* [48]. It is noteworthy here that the composite nucleus is in the excitation energy range from 30 to 50 MeV, hence its shell structure probably has been washed out during the fusing process. Moreover, as pointed out by Świątecki *et al.* [15], shell effects in asymmetric fission saddle mass are expected to be small. In view of these facts, the shell structure is not taken into account in the fusion probability calculations. The comparison of our approach with the measured ER cross sections in Fig. 3 may indicate that the effects of shell structure and deformations of the reaction partners on the ER cross sections are limited at this stage of the process.

The production cross sections of $^{299,298}\text{120}$ isotopes produced in the $^{58}\text{Fe} + ^{244}\text{Pu}$ fusion-evaporation reaction are presented in Fig. 4. It is found that the maximum ER cross sections in $3n$ and $4n$ evaporation channels of the $^{58}\text{Fe} + ^{244}\text{Pu}$ reaction are 0.005 and 0.016 pb, respectively. The dashed lines are the results of Zagrebaev *et al.* [49], which are about two times smaller than our prediction. In terms of the dinuclear system

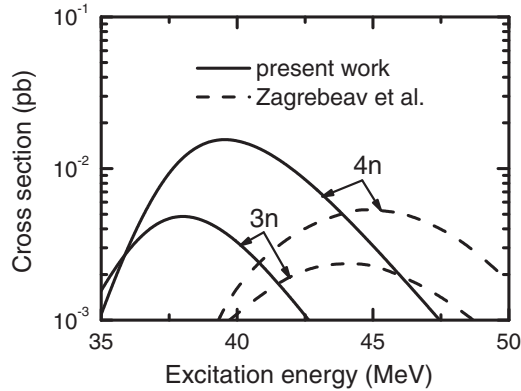


FIG. 4. Predicted evaporation residue cross sections for the $3n$ and $4n$ evaporation channels in the $^{58}\text{Fe} + ^{244}\text{Pu}$ reaction leading to the formation of $^{299}\text{120}$ and $^{298}\text{120}$ isotopes. Dashed lines are the prediction of Zagrebaev *et al.* [49].

model, very recently Wang *et al.* [25] made an evaluation of the ER cross sections for the system $^{58}\text{Fe} + ^{244}\text{Pu}$ and claimed that the maximal value in the $4n$ channel is only about 4 fb.

In summary, we have calculated the ER cross sections for $3n$ and $4n$ evaporation channels in the $^{58}\text{Fe} + ^{244}\text{Pu}$ reaction

leading to the formation of $^{299}\text{120}$ and $^{298}\text{120}$ isotopes by means of the modified FBD model. In the model, dynamic evolution from dinucleus to mononucleus is taken into account with two-dimensional coupled Langevin equations. In this way, the distribution of the injection distance in the asymmetric fission valley is determined in the fusion probability calculations. The calculated maximum ER cross sections in $3n$ and $4n$ evaporation channels of the $^{58}\text{Fe} + ^{244}\text{Pu}$ reaction are, respectively, 0.005 and 0.016 pb, which are far below the present experimental sensitivity for the detection of one decay. The fusion probability calculated with the modified FBD model clearly shows that fusion of the heavy system $^{58}\text{Fe} + ^{244}\text{Pu}$ is severely hindered. However, in order to synthesize SHEs with $Z \geq 120$, projectiles heavier than ^{48}Ca have to be used. Therefore, further investigation of the fusion of heavy reaction systems is greatly needed both theoretically and experimentally.

This work was supported by the “985 project” (Grant No. 98507-012009) and “211 project” of the Ministry of Education of China, the National Natural Science Foundation of China (Grant No. 11074312), and Fundamental Research Funds for the Central Universities (Grant No. 1112KYQN35).

- [1] S. Hofmann and G. Münzenberg, *Rev. Mod. Phys.* **72**, 733 (2000); S. Hofmann *et al.*, *Eur. Phys. J. A* **10**, 5 (2001).
- [2] K. Morita *et al.*, *J. Phys. Soc. Jpn.* **76**, 043201 (2007); **76**, 045001 (2007).
- [3] Yu. Ts. Oganessian, V. K. Utyonkoy, Yu. V. Lobanov *et al.*, *Phys. Rev. Lett.* **83**, 3154 (1999); Yu. Ts. Oganessian *et al.*, *Nature* **400**, 242 (1999).
- [4] Yu. Ts. Oganessian *et al.*, *Phys. Rev. C* **69**, 054607 (2004).
- [5] Yu. Ts. Oganessian *et al.*, *Phys. Rev. C* **70**, 064609 (2004).
- [6] Yu. Ts. Oganessian *et al.*, *Phys. Rev. C* **72**, 034611 (2005); **69**, 021601(R) (2004).
- [7] Yu. Ts. Oganessian *et al.*, *Phys. Rev. C* **74**, 044602 (2006).
- [8] Yu. Ts. Oganessian *et al.*, *Phys. Rev. Lett.* **104**, 142502 (2010).
- [9] P. Moller, J. R. Nix, W. D. Myers, and W. J. Swiatecki, *At. Data Nucl. Data Tables* **59**, 185 (1995).
- [10] A. Sobiczewski and K. Pomorski, *Prog. Part. Nucl. Phys.* **58**, 292 (2007).
- [11] M. Bender *et al.*, *Phys. Lett. B* **515**, 42 (2001); P. Ring, *Prog. Part. Nucl. Phys.* **37**, 193 (1996); M. Bender, P. H. Heenen, and P. G. Reinhard, *Rev. Mod. Phys.* **75**, 121 (2003).
- [12] J. Meng, H. Toki, S. Zhou, S. Zhang, W. Long, and L. Geng, *Prog. Part. Nucl. Phys.* **58**, 292 (2007).
- [13] Yu. Ts. Oganessian *et al.*, *Phys. Rev. C* **79**, 024603 (2009).
- [14] W. J. Świątecki, K. Siwek-Wilczyńska, and J. Wilczyński, *Acta Phys. Pol. B* **34**, 2049 (2003).
- [15] W. J. Świątecki, K. Siwek-Wilczyńska, and J. Wilczyński, *Phys. Rev. C* **71**, 014602 (2005).
- [16] Z. H. Liu and J. D. Bao, *Phys. Rev. C* **81**, 044606 (2010).
- [17] Z. H. Liu and J. D. Bao, *Phys. Rev. C* **83**, 044613 (2011).
- [18] T. Cap, K. Siwek-Wilczyńska, and J. Wilczyński, *Phys. Rev. C* **83**, 054602 (2011).
- [19] V. I. Zagrebaev, *Phys. Rev. C* **64**, 034606 (2001).
- [20] V. I. Zagrebaev, Y. Aritomo, M. G. Itkis, Yu. Ts. Oganessian, and M. Ohta, *Phys. Rev. C* **65**, 014607 (2001).
- [21] D. Boilley, H. Lü, C. W. Shen, Y. Abe, and B. G. Giraud, *Phys. Rev. C* **84**, 054608 (2011).
- [22] W. Li, N. Wang, J. F. Li, H. Xu, W. Zuo, E. Zhao, J. Q. Li, and W. Scheid, *Europhys. Lett.* **64**, 750 (2003).
- [23] W. Li, N. Wang, F. Jia, H. Xu, W. Zuo, Q. Li, E. Zhao, J. Li, and W. Scheid, *J. Phys. G* **32**, 1143 (2006).
- [24] N. Wang, J.-Q. Li, and E.-G. Zhao, *Phys. Rev. C* **78**, 054607 (2008).
- [25] N. Wang, E. G. Zhao, W. Scheid, and S. G. Zhou, *Phys. Rev. C* **85**, 041601(R) (2012).
- [26] G. Nuhn, W. Scheid, and J. Y. Park, *Phys. Rev. C* **35**, 2146 (1987).
- [27] A. Diaz-Torres, *Phys. Rev. Lett.* **101**, 122501 (2008).
- [28] V. I. Zagrebaev, Yu. Ts. Oganessian, M. G. Itkis, and Walter Greiner, *Phys. Rev. C* **73**, 031602(R) (2006).
- [29] C. Y. Wong, *Phys. Rev. Lett.* **31**, 766 (1973).
- [30] K. Nishio *et al.*, *Phys. Rev. C* **82**, 024611 (2010).
- [31] J. R. Nix, *Nucl. Phys. A* **130**, 241 (1969).
- [32] H. J. Krappe, J. R. Nix, and A. J. Sierk, *Phys. Rev. Lett.* **42**, 215 (1979); *Phys. Rev. C* **20**, 992 (1979).
- [33] A. J. Sierk, *Phys. Rev. C* **33**, 2039 (1986).
- [34] J. Blocki, Y. Bonch, J. R. Nix, J. Randrup, M. Robel, A. J. Sierk, and W. J. Swiatecki, *Ann. Phys.* **113**, 330 (1978).
- [35] J. Randrup and W. J. Swiatecki, *Ann. Phys.* **124**, 193 (1980).
- [36] A. K. Dhara, K. Krishan, C. Bhattacharya, and S. Bhattacharya, *Phys. Rev. C* **57**, 2453 (1998).
- [37] S. M. Mirfathi and M. R. Pahlavani, *Phys. Rev. C* **78**, 064612 (2008).
- [38] P. Fröbrich and I. I. Gontchar, *Phys. Rep.* **292**, 131 (1998).
- [39] K. T. R. Davies, A. J. Sierk, and J. R. Nix, *Phys. Rev. C* **13**, 2385 (1976).
- [40] Y. Abe, D. Boilley, G. Kosenko, and C. W. Shen, *Acta Phys. Pol. B* **34**, 2091 (2003).
- [41] W. J. Swiatecki, *Phys. Scripta* **24**, 113 (1981).

- [42] Z. H. Liu and J. D. Bao, [Phys. Rev. C **80**, 034601 \(2009\)](#).
- [43] R. Vandenbosch and J. R. Huizenga, *Nuclear Fission* (Academic Press, New York, 1973), p. 233.
- [44] K. Siwek-Wilczyńska, I. Skwira, and J. Wilczyński, [Phys. Rev. C **72**, 034605 \(2005\)](#).
- [45] Yu. Oganessian, *J. Phys. G: Nucl. Part. Phys.* **34**, R165 (2007).
- [46] A. V. Ignatyuk, G. N. Smirenkin, and A. S. Tishin, *Yad. Fiz.* **21**, 485 (1975) [*Sov. J. Nucl. Phys.* **29**, 255 (1975)].
- [47] W. Reisdorf, [Z. Phys. A **300**, 227 \(1981\)](#).
- [48] V. I. Zagrebaev, M. G. Itkis, and Yu. Ts. Oganessian, [Phys. At. Nucl. **66**, 1033 \(2003\)](#).
- [49] V. I. Zagrebaev and W. Greiner, [Phys. Rev. C **78**, 034610 \(2008\)](#).